

Contribution from the Institute of Aquatic Sciences, EAWAG/ETH, 8600 Dübendorf, Switzerland, and Laboratory for Physical Chemistry, ETH Zentrum, 8092 Zuerich, Switzerland

Interactions of Chromium(III) Complexes with Hydrated δ -Al₂O₃: Rearrangements in the Coordination Sphere Studied by Electron Spin Resonance and Electron Spin-Echo Spectroscopies

R. Karthein,[†] H. Motschi,[‡] A. Schweiger,^{*†} S. Ibric,[‡] B. Sulzberger,[‡] and W. Stumm[†]

Received March 27, 1990

Chromium(III) complex binding mechanisms to hydrated δ -Al₂O₃ are investigated by applying ESR and ESEEM spectroscopies. Adsorption isotherms of the Cr(H₂O)₆³⁺ and the Cr(oxalate)₃³⁻ complexes can be monitored adequately either by conventional analysis (AAS) or by measuring the spin concentration of the adsorbed species. Because of the inertness of chromium(III) species, time-resolved changes of ligand exchange reactions can be identified. Optical reflectance and ESR spectra indicate the gradual transition from outer-sphere to inner-sphere binding mechanisms. In the case of the Cr(H₂O)₆³⁺ ion, hydrolysis and/or polynuclear complex formation are potential competitive reactions, whereas for the precursor complex Cr(oxalate)₃³⁻ no hydrolyzable functional groups are present. For the latter example, an initially charge-reversed (anionic) type of isotherm gradually interconverts into a cationic type yet is different from that of the aquo complex.

Introduction

Adsorption/desorption equilibria of transition-metal ions follow distinct patterns as functions of pH.¹ A sharp increase in adsorption of the metal ion is accompanied by a simultaneous release of protons. The "surface complex formation model" of Stumm and Schindler¹ assumes that protonation is a competitive reaction and that the number of protons released correlates with the number of surface hydroxyl groups involved in the metal binding. The so-called "hydrolysis model" of James and Healy² postulates the adsorption of a hydrolyzed metal aquo ion, Me(OH)_n^{(z-n)+}, at the (negatively charged) electric double layer. Although the two mechanisms are thermodynamically indistinguishable, recent kinetic investigations and spectroscopic studies on copper(II)³ have given evidence for surface complexation.

Chromium is an element of significance in geochemical cycles and an important trace element in nutrition⁴ and belongs to those elements that are dominated by scavenging in the deep-sea concentration profiles; however, whether this is due to hydrolysis or to surface complexation remains an open question.⁵ Chromium(III) is assumed to enter the surface layers of the oceans by biological reduction and/or photoreduction of the chromate(VI) ion, which is the prevalent oxidation state of this heavy metal in the ocean redox boundaries.⁶ Furthermore, chromium(III) aquo ions show a peculiar behavior with respect to adsorption. They are kinetically inert (ligand exchange reactions with $t_{1/2} \sim 10^7$ s) and have a strong tendency to form polynuclear hydroxo species. Thus, Cr(III) provides an excellent model system to study the kinetic sequences of hydrolysis vs ligand exchange and polymerization.

Discrete site complexation of transition-metal ions (Cu(II), Cr(III), Mn(II)) and the rare earth element Nd(III) has been recently identified by ESR (electron spin resonance) spectroscopy on the surface of hydrated aluminum oxide (δ -Al₂O₃),⁷ on the bacterium *Klebsiella pneumoniae*,⁸ on the sulfate polystyrene Latex,⁹ and on the carbonate mineral siderite.^{10,11} The d³ electron system of chromium(III) is also suitable to ESEEM (electron spin-echo envelope modulation) measurements, which are known to be sensitive to magnetic nuclei in the coordination sphere (¹H of water ligands and ²⁷Al of surface Al-O functional groups).

In this article we present the results of an ESR and ESEEM study of inner-sphere and outer-sphere chromium surface complexes in combination with the corresponding adsorption isotherm and with some kinetic considerations. A comparison between the two precursor solution complexes Cr(H₂O)₆³⁺ and Cr(oxalate)₃³⁻ is expected to provide an insight into potential differences of the adsorption mechanism with respect to hydrolysis effects in the former case and pure ligand exchange reactions in the latter case.

Materials and Methods

Sample Preparation. Commercial δ -Al₂O₃ ("Aluminiumoxid C", Degussa, Frankfurt) was used as a surfactant-free suspension in deionized water (10 g/L) without pretreatment. K₃Cr(C₂O₄)₃ was prepared by stoichiometric mixture of Cr(NO₃)₃ (Merck, Darmstadt) and K₂(C₂O₄) (Merck, Darmstadt) heat treated at 60 °C for 8 h. The adsorption was achieved by first acidifying the aluminum suspension with 0.1 M HNO₃ to a pH of about 2.5. Constant ionic strength of 0.1 M was reached by the addition of KNO₃. The experiment was started by the addition of free chromium ions or of chromium oxalato complex (both 30 mM stock solutions) to the aluminum suspension. Then, the pH was adjusted by 0.1 M KOH and held constant at the desired pH values during the experiment with an automatic buret (Metrohm 665). The final volume was 100 mL with [Cr³⁺]_{tot} of 0.5, 1, 2, and 3 mM. Each experiment was run for several months, during which 10-mL aliquots of suspension were regularly taken with a syringe and filtered through a 0.01- μ m pore size cellulose nitrate Sartorius filter. The filter was then quickly dried on a tissue paper, rolled into an ESR tube, and stored at -18 °C. The filtrate was analyzed with a Perkin Elmer Model 5000 atomic absorption spectrophotometer.

No difference in the ESR results was found for samples that were centrifuged and dried for 1/2 hour at 40 °C. These dried samples were used for measurements of the electronic spectra of the metal surface complexes.

Electronic Spectra. Electronic spectra were measured at room temperature with a UVIKON 860 UV/vis spectrophotometer from Kontron Instruments. Reflectance measurements of the surface complex species were made with Ulbricht cube equipment. The sample used for this work was compacted by pressing the dried powder into a disk.

ESR Measurements. Two spectrometers were used. The continuous wave ESR spectra were recorded between liquid helium and room temperatures on an ESP 300 system from Bruker. All spectra were measured at a microwave frequency of 9.44 GHz, a microwave power of 2 mW, a modulation amplitude of 0.5 mT, and a modulation frequency of 100 kHz. The *G* values and the line widths were determined with a Bruker

- (1) Schindler, P. W.; Stumm, W. In *Aquatic Surface Chemistry*; Stumm, W., Ed.; John Wiley & Sons: New York, 1987; p 83.
- (2) James, R. O.; Healy, T. W. *J. Colloid Interface Sci.* **1972**, *40*, 42.
- (3) Hachiya, K.; Sasaki, M.; Saruta, Y.; Mikami, N.; Yasunaga, T. *J. Phys. Chem.* **1984**, *88*, 23.
- (4) Müller, A.; Diemann, E.; Sassenberg, P. *Naturwissenschaften* **1988**, *75*, 155.
- (5) Whitfield, M.; Turner, D. R. In *Aquatic Surface Chemistry*; Stumm, W., Ed.; John Wiley & Sons: New York, 1987; p 457.
- (6) Murray, J. W.; Spell, B.; Paul, B. In *Trace Metals in Seawater*; Wong, C. S.; Boyle, E. A.; Bruland, K. W.; Burton, J. D.; Goldberg, F. D., Eds.; Plenum: New York, 1986; p 643.
- (7) Möhl, W.; Motschi, H.; Schweiger, A. *Inorg. Chem.* **1990**, *29*, 1536.
- (8) Möhl, W.; Motschi, H.; Schweiger, A. *Langmuir* **1988**, *4*, 580.
- (9) Charlet, L.; Karthein, R. *Aquat. Sci.* **1990**, *52*, 93.
- (10) Wersin, P.; Charlet, L.; Karthein, R.; Stumm, W. *Geochem. et Cosmochim. Acta* **1989**, *53*, 2787.
- (11) Bruno, J.; Charlet, L.; Carrol, S.; Karthein, R.; Sandino, A.; Wersin, P. In *Water-Rock Interaction*; Miles, D. L., Ed.; Balkema: Rotterdam, The Netherlands, 1989; p 121.

[†]ETH Zentrum.
[‡]EAWAG/ETH.

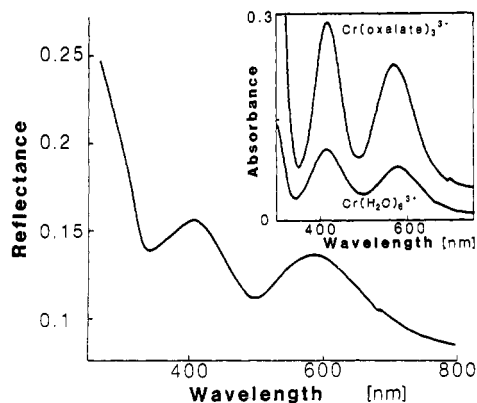


Figure 1. Vis reflectance spectrum of $[\text{Cr}(\text{oxalate})_3]^{3-}$ equilibrated for 14 days on δ -Al₂O₃. Inset: Electronic spectra of $\text{Cr}(\text{H}_2\text{O})_6^{3+}$ and $[\text{Cr}(\text{oxalate})_3]^{3-}$ in solution.

Table I. Band Peaks of the Electronic Spectra in the Visible Region of Different Chromium Complexes (Wavelength in nm \pm 3 nm)

| | $\text{Cr}(\text{H}_2\text{O})_6^{3+}$ | | $[\text{Cr}(\text{oxalate})_3]^{3-}$ | |
|-------------------------|--|-----------------|--------------------------------------|-----------------|
| | solution | surface complex | solution | surface complex |
| λ_{min} | 341 | 338 | 351 | 339 |
| λ_{max} | 409 | 408 | 420 | 410 |
| λ_{min} | 496 | 499 | 487 | 498 |
| λ_{max} | 576 | 579 | 570 | 580 |
| λ_{forb} | 668 | 672 | 697 | 684 |

NMR Gaussmeter and DPPH as a *G* marker. The spin concentration of the paramagnetic Cr(III) species was estimated by double integration of the ESR signal.

ESEEM measurements were carried out on a home-built spectrometer¹² equipped with a fast pulse sequence generator and a bridged loop-gap resonator.¹³ In all experiments, the two-pulse echo sequence with pulse lengths at 10–20 ns was used. The time increment was 10 ns; the pulse repetition rate, 1 kHz. All ESEEM signals were recorded at liquid helium temperature.

Results

UV/Vis Spectra. Figure 1 shows the solid-state reflectance spectrum in the visible region of $\text{Cr}(\text{oxalate})_3^{3-}$ that was equilibrated for 14 days on the δ -Al₂O₃ surface. The spectrum yields clear absorbance for the two allowed band maxima at 410 and 580 nm and the observable forbidden transition at 684 nm. The spectrum is very similar to the spectrum of the $\text{Cr}(\text{H}_2\text{O})_6^{3+}$ ions adsorbed on the surface after 4 days of equilibration (data not shown). Electronic spectra of $\text{Cr}(\text{H}_2\text{O})_6^{3+}$ and $\text{Cr}(\text{oxalate})_3^{3-}$ complexes in solution are shown in the inset of Figure 1. The peak positions of the $\text{Cr}(\text{oxalate})_3^{3-}$ spectrum are in excellent agreement with the data published by Eaton et al.¹⁴

Table I shows that the band positions of the two chromium surface complexes are very similar. In the case of *d*³ ions, the ligand field strength is given by the spin-allowed *d*-*d* transition (⁴A_{2g} - ⁴T_{2g}), assigned to the peak with λ_{max} at about 580 nm.¹⁵ The shift of this transition wavelength indicates that the ligand field strength of the chromium surface complexes decreases.

ESR Spectra of $\text{Cr}(\text{H}_2\text{O})_6^{3+}$ in Aqueous Solution and on the Surface of Hydrated δ -Al₂O₃. The ESR spectrum of Cr(III) aquo ions in frozen solution at 153 K is shown in Figure 2a. It consists of one resonance line at *g* = 1.97 with a width of 4.4 mT. When the sample was cooled to liquid helium temperature, no change of the line shape was observed. Only the signal intensity increases according to Boltzmann distribution.

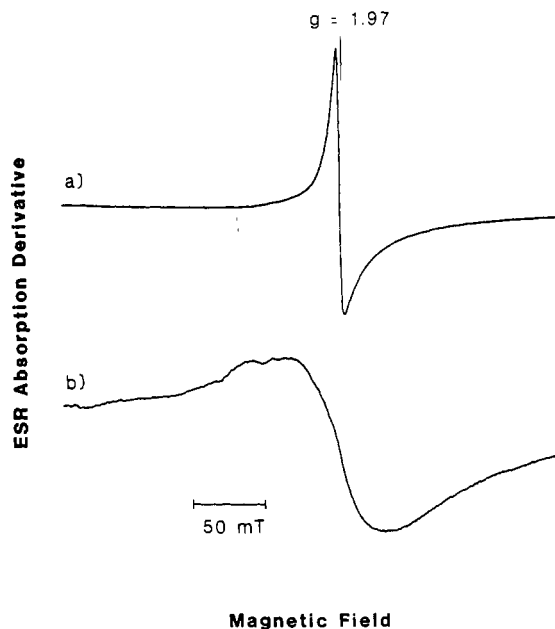


Figure 2. (a) ESR spectrum of $\text{Cr}(\text{H}_2\text{O})_6^{3+}$ in aqueous solution. (b) ESR spectrum of the $\text{Cr}(\text{aq})^{3+}$ complex fragment adsorbed on the δ -Al₂O₃ surface.

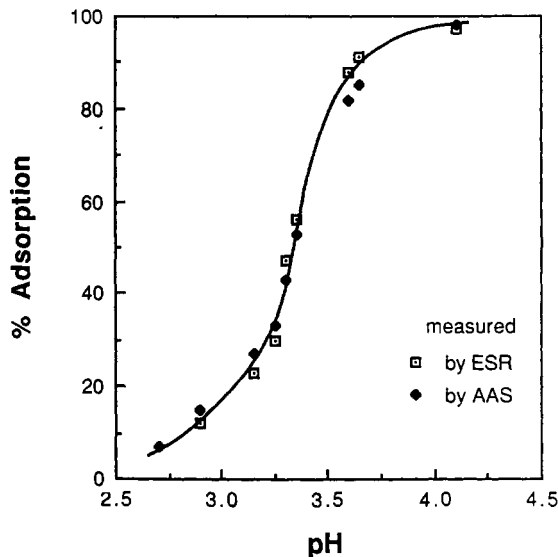


Figure 3. Adsorption isotherms of Cr(III) on δ -Al₂O₃ measured via the spin concentration of the ESR signal (\square) and by AAS (\blacklozenge).

The ESR spectrum of Cr(III) aquo ions adsorbed on δ -Al₂O₃ remains silent during several hours after mixing the suspension. However, a prolonged equilibration time of several days leads to a broad chromium signal near *g* = 2.0 with a line width of 63 mT (Figure 2b). It was found that this line width is depending on $[\text{Cr}^{3+}]_{\text{tot}}$ on the surface. The line width broadens from 58 to 105 mT by increasing $[\text{Cr}^{3+}]_{\text{tot}}$ from 0.5 to 3 mM, corresponding to a surface loading of 0.16 to 1 of the exchange capacity. The same dependence of the signal intensity in solution was found upon cooling the sample to liquid helium temperature.

The adsorption isotherm of the metal ions measured by the spin concentration of the ESR signal (Figure 3) increases with increasing pH. The thermodynamic adsorption isotherm of Cr(III) on the δ -Al₂O₃ surface as measured by atomic absorption spectroscopy (AAS) of the filtrate (Figure 3) parallels strictly the adsorption isotherm determined from the spin concentrations.

ESR of the Cr(III) Oxalato Complex in Solution and on the Surface of δ -Al₂O₃. The ESR spectrum of a frozen solution of $[\text{Cr}(\text{C}_2\text{O}_4)_3]^{3-}$ with *g* values of 5.86, 3.72, and 1.97 corresponding to a slightly orthorhombic ligand field symmetry (*E/D* ~ 0.1) is shown in Figure 4a. The line shape and the rhombicity are

- (12) Fauth, J. M.; Schweiger, A.; Braunschweiler, L.; Forrer, J.; Ernst, R. *R. J. Magn. Reson.* **1986**, *66*, 74.
 (13) Pfenninger, S.; Forrer, J.; Schweiger, A.; Weiland, Th. *Rev. Sci. Instrum.* **1988**, *59*, 752.
 (14) Eaton, S. S.; Yager, T. D.; Eaton, G. R. *J. Chem. Educ.* **1976**, *56*, 635.
 (15) Purcell, K. F.; Klotz, J. C. *Inorganic Chemistry*; Saunders: Philadelphia, 1977; p 564.

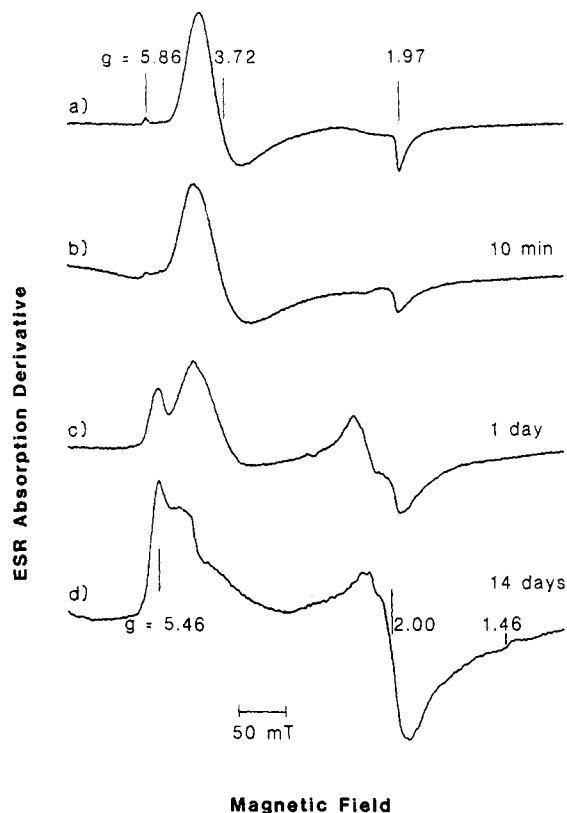


Figure 4. ESR spectra of $[\text{Cr}(\text{oxalate})_3]^{3-}$: (a) contained in frozen solution; (b–d) adsorbed on the $\delta\text{-Al}_2\text{O}_3$ surface at pH 4.2 for three different equilibration times, 10 min (b), 1 day (c), and 14 days (d).

in agreement with the measured data of chromium acetylacetonate in 1-butanol.¹⁶ The ESR parameters do not change when the metal complex is adsorbed on $\delta\text{-Al}_2\text{O}_3$ for a short time only (<4 h) (Figure 4b). For an equilibration time of the order of 1 day, the ESR spectrum transfers to a set of signals that can be attributed to several chromium species. Parts c and d of Figure 4 demonstrate the superposition of two major new ESR signals in addition to the signal of $[\text{Cr}(\text{C}_2\text{O}_4)_3]^{3-}$: one signal with a strong orthorhombic distortion ($E/D \sim 0.333$; $g = 5.46, 2.00, 1.46$) and one broad signal at $g = 2.0$ with a line width of 50 mT. The latter closely resembles the spectrum of chromium aquo ions adsorbed on $\delta\text{-Al}_2\text{O}_3$ (Figure 2b). The intensity of both spectra increases with time. When equilibration is completed after 14 days, the spectrum given in Figure 4d is observed.

This variation of the ESR spectrum is accompanied by a corresponding change in the adsorption behavior. The amount of metal complex adsorbed on $\delta\text{-Al}_2\text{O}_3$ shown in Figure 5 is measured via the spin concentration of the signal with $E/D \sim 0.1$. The adsorption is strongly dependent on the equilibration time and on pH. In contrast to the adsorption of the free chromium aquo ions (Figure 3), the adsorption of the complexed chromium decreases with increasing pH during the first few hours. After 1 day of equilibration, the adsorption at the lower pH edge decreases and remains nearly constant in the measured pH range. Finally, an equilibration time of 14 days causes an inversion of the adsorption characteristics as a function of pH, in agreement with the change of the ESR signals shown in Figure 4. The amount of metal complex adsorbed on $\delta\text{-Al}_2\text{O}_3$ is measured via the spin concentration of the signal with $E/D \sim 0.333$ and the broad signal at $g = 2$. The adsorption isotherm shows a "cation-like" slope corresponding to the adsorption of Cr(III) aquo ions (Figure 3).

ESEEM of the Cr(III) Aquo and the Cr(III) Oxalato Complexes in Frozen Solution. The two-pulse echo modulation pattern and the corresponding Fourier transform ESEEM spectra of the Cr(III) aquo and the Cr(III) oxalato complexes in frozen solution

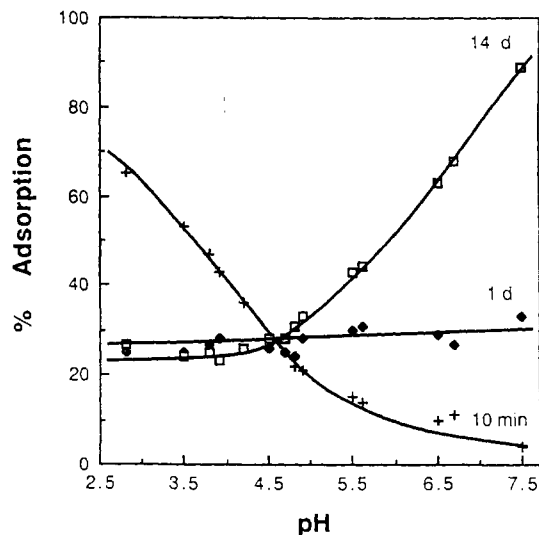


Figure 5. Time-dependent change of the adsorption isotherm of $[\text{Cr}(\text{oxalate})_3]^{3-}$ on $\delta\text{-Al}_2\text{O}_3$ measured via the respective spin concentration of the corresponding ESR signals attributed to the different surface complexes.

are shown in Figure 6. Both spectra are quite similar and are dominated by the strong peak at the proton Larmor frequency of 14 MHz and the sum peak at 28 MHz. These two frequencies are typical for remote water protons.⁷ The proton hyperfine couplings of water directly coordinated to a metal ion are usually not observable in ESEEM spectroscopy. This is due to the fact that the dipolar interaction of such protons is quite large. In the Cu(II) aquo complex, for example, the largest dipolar coupling obtained from single-crystal ENDOR data is 10.6 MHz.¹⁷ In $\text{Cu}(\text{H}_2\text{O})_6^{2+}$ in frozen solution, this anisotropy results in broad hyperfine lines with echo modulations in the time domain decaying within the dead time of the spectrometer.¹⁸ Thus, the only remaining features in the two-pulse spectrum are again peaks at the proton Larmor frequency ν_H and at $2\nu_H$.⁷ Since the metal ion–oxygen distances in $\text{Cu}(\text{H}_2\text{O})_6^{2+}$ are close to the one found in $\text{Cr}(\text{H}_2\text{O})_6^{3+}$,¹⁹ also, in the Cr(III) complexes, protons of directly coordinated water may not be measured with ESEEM.

ESEEM of the Cr(III) Surface Complexes. The surface complex formed after addition of $\text{Cr}(\text{H}_2\text{O})_6^{3+}$ and $[\text{Cr}(\text{oxalate})_3]^{3-}$ to a suspension of $\delta\text{-Al}_2\text{O}_3$ were also studied by means of two-phase ESEEM. In the case of $\text{Cr}(\text{H}_2\text{O})_6^{3+}$ initially adsorbed on the surface, no electron spin echo could be detected as a consequence of the missing ESR signal at low pH. On the other hand, the ESEEM pattern of $[\text{Cr}(\text{oxalate})_3]^{3-}$ adsorbed on $\delta\text{-Al}_2\text{O}_3$ shows a characteristic change with increasing equilibration time analogous to the signal changes of the continuous wave ESR spectra (Figure 4).

Figure 7 depicts the two-pulse ESEEM pattern and ESEEM spectrum of the same sample as in Figure 4b with the ESR observer at $g = 2$. Note that the echo decay for the surface complex is much faster than the one for the chromium complex in solution. In addition to the proton frequencies observed in solution, the ESEEM pattern shows two significant peaks at 3.7 and 7.4 MHz. They represent the nuclear Zeeman frequency and twice this frequency of the ^{27}Al nuclei of $\delta\text{-Al}_2\text{O}_3$, indicating the close proximity between surface and chromium ions.

When the Cr(III) aquo and Cr(III) oxalato complex are equilibrated and adsorbed for several days on $\delta\text{-Al}_2\text{O}_3$, the two-pulse ESEEM results of both of them are similar (Figure 8). Remember that the proton ESEEM is only sensitive to remote water. The echo intensity in this case decays even faster than that of the precursor complex. This can best be interpreted as being

(17) Atherton, N. M.; Horsewill, A. J. *Mol. Phys.* **1979**, *37*, 1349.

(18) Schweiger, A. In *Advanced EPR*; Hoff, A. J., Ed.; Elsevier: Amsterdam, 1989; p 243.

(19) Sham, T. K.; Hastings, J. B.; Perlman, M. L. *Chem. Phys. Lett.* **1981**, *83*, 391.

(16) Doeuff, S.; Henry, M.; Sanchez, C.; Livage, J. *J. Non-Cryst. Solids* **1987**, *89*, 84.

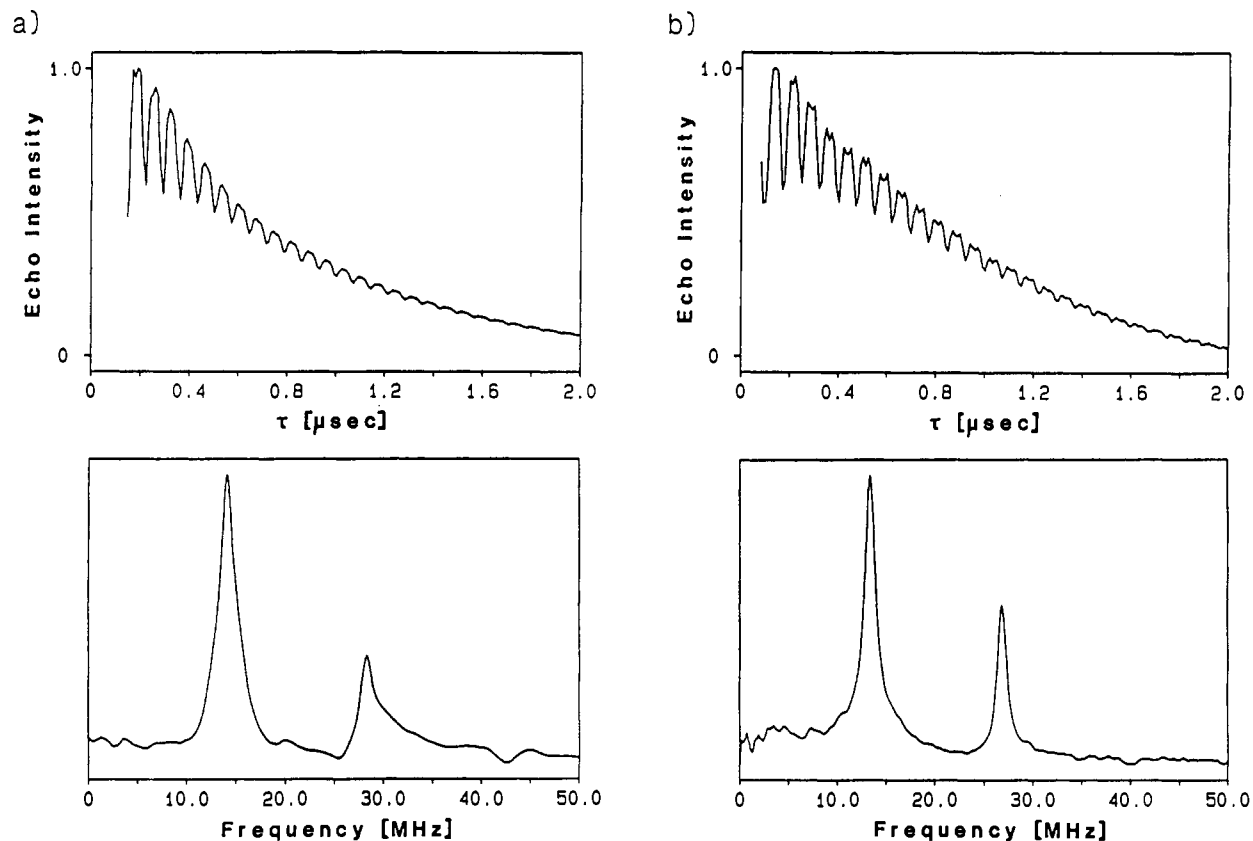


Figure 6. Two-pulse ESEEM patterns and corresponding ESEEM spectra of (a) $\text{Cr}(\text{H}_2\text{O})_6^{3+}$ and (b) $[\text{Cr}(\text{C}_2\text{O}_4)_3]^{3-}$ in frozen solution (observer position at $g = 2$).

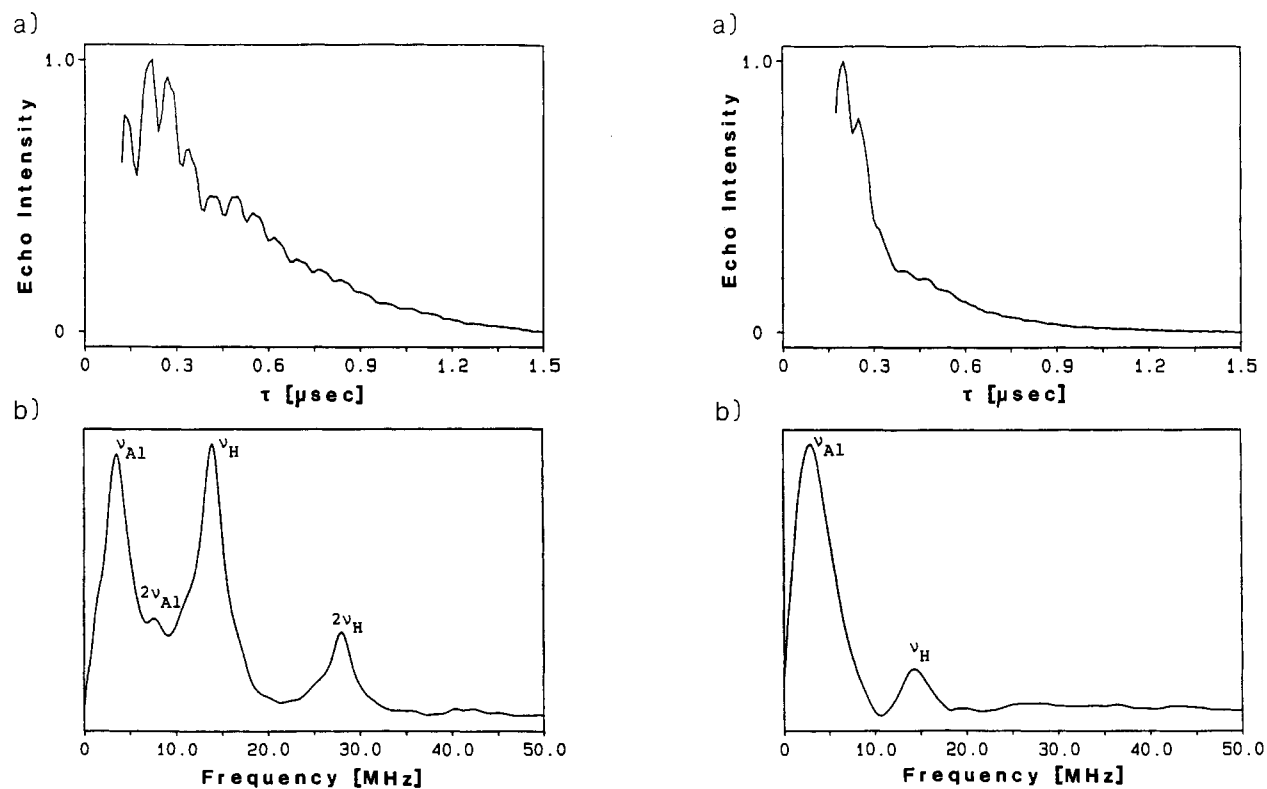


Figure 7. (a) Two-pulse ESEEM pattern of the chromium species adsorbed on the δ -Al₂O₃ surface after 10 min of equilibration with $[\text{Cr}(\text{C}_2\text{O}_4)_3]^{3-}$ (pH 4.2, compare ESR spectrum of Figure 4b) (observer position at $g = 2$). (b) Corresponding ESEEM spectrum.

Figure 8. (a) Two-pulse ESEEM pattern of the chromium species adsorbed on the δ -Al₂O₃ surface after 14 days of equilibration with $[\text{Cr}(\text{C}_2\text{O}_4)_3]^{3-}$, indicating the existence of $[\text{Cr}(\text{C}_2\text{O}_4)_x]^{(3-2x)}$ ($x = 1, 2$) and the $[\text{Cr}(\text{aq})]^{3+}$ fragment bond to the surface (pH 4.2, compare ESR spectrum of Figure 4d) (observer position at $g = 2$). (b) Corresponding ESEEM spectrum.

due to the dipolar interaction of Cr-Cr on neighboring sites. A quite analogous situation is found in the spectrum of Cu(II) on δ -Al₂O₃.⁷ The striking observation in the ESEEM spectrum, however, is the drastic decrease of the proton peak intensity relative

to the intensity of the aluminum peak. The sum peak of the protons has disappeared.

Discussion

Chromium(III) complexes are characterized by their inertness toward ligand exchange reactions. However, several studies on the hydrolysis of the Cr(III) aquo ion have shown that dinuclear and polynuclear hydroxo species are formed with increasing pH.^{20,21} Therefore, ligand exchange with surface functional groups of δ -Al₂O₃ is a competitive reaction in hydrolysis/polymerization.

ESR spectroscopy elucidates the coordination sphere of paramagnetic Cr(III) and is a powerful tool to characterize distortions of the ligand field, caused by hydrolysis, polymerization,²² and binding to surfaces.^{9,23} Cr(III) has three unpaired electrons ($S = 3/2$) and exhibits a zero field splitting that is very sensitive to small variations of the coordination sphere.²⁴ It has a strong preference for octahedral coordination as a result of the ligand field stabilization energy of the d³ electron configuration. Furthermore, a Cr(III) ion has a ⁴F singlet ground state, so that broadening of the ESR line shape due to an interaction with a low-lying excited state is generally negligible. According to the studies of chromium compounds on silica gels²⁵ and chromium surface complexes in the presence of inorganic ligands,⁹ broadening of the line width is mainly attributed to the changes of the relaxation time and the electron spin-spin interactions between the metal ions adsorbed on the surface.

When the Cr(III) aquo ion was adsorbed on the surface, a drastic increase of the ESR line width was observed, depending on the chromium concentration on the surface. This line broadening effect is typical of an increased dipolar interaction upon approaching higher surface coverage and/or heterogeneity of local symmetry; a phenomenon that was also observed for Cu²⁺⁷ and VO²⁺²⁶ adsorbed on the same surface. A similar broadening is also found in chromium hydroxy polymer formation.^{9,22} In both cases, spin-spin interaction between the metal ions causes the broad ESR lines. On the other hand, it is known that the line width of Cr(III) polymers changes dramatically upon cooling to low temperatures.²² The ESR signal of Cr(III) adsorbed on the surface, as shown in Figure 2b, however, is not significantly temperature-dependent. On the basis of these arguments, it is concluded that chromium complexation at specific surface sites rather than chromium polymers formation takes place. This is supported by the finding that the line width increases for shorter Cr(III)-Cr(III) distances in correspondence to the increase of the metal concentration on the surface.²⁷

The initial adsorption step of a Cr(III) aquo ion is dominated by an electrostatic interaction, as was shown by Stumm et al.²⁸ for the Co(III) adsorption of inert Co(NH₃)₅·H₂O complex. A typical shape of the adsorption isotherm measured by ESR and AAS is displayed in Figure 3 and is characteristic for a cation adsorption onto a hydrous oxide surface whose density of anionic sites augments with increasing pH. In order to circumvent the competitive hydrolysis of the Cr(III) aquo ion, the Cr(III) tris(oxalato) complex was chosen as a precursor to adsorption. The reflectance spectrum (Figure 1) shows that the chromium surface complexes formed with the metal complex and δ -Al₂O₃ is subject to a change in the molecular structure by increasing the equilibration time. The shift of the band maximum for the ⁴A₂-⁴T₂ transition is indicative for the decrease of the ligand field strength, when a specific surface complex formation takes place.²⁹

More instructive insights into the molecular structure and dynamics of interactions between chromium and the specific surface sites are given by ESR methods. The ESR spectra (Figure 4) indicate ligand movements in the first coordination sphere of

Chart I. Proposed Cr(III) Outer-Sphere Surface Complex Formation

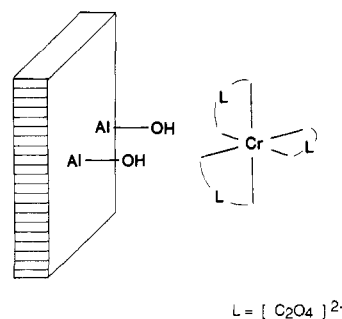
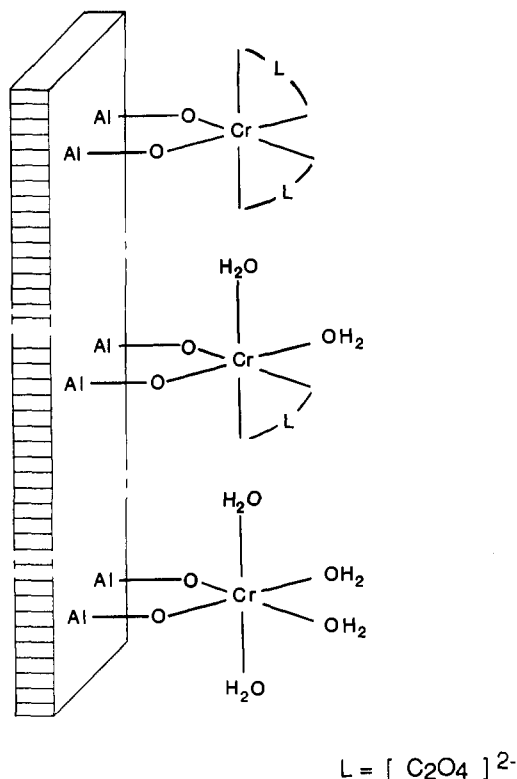


Chart II. Proposed Cr(III) Inner-Sphere Surface Complexes Formation



the chromium ion dependent on the equilibration time. The ESR signal of Cr(oxalate)₃³⁻ in solution and the signal obtained after adsorption of this species on δ -Al₂O₃ after a short equilibration time are very similar (Figure 4a,b). This indicates that the ligand field remains intact and therefore an outer-sphere adsorption complex is formed. On the other hand, the signal with strong orthorhombic symmetry ($E/D \sim 0.333$) as shown in Figure 4c,d was also observed for Cr(oxalate)₂⁻ and Cr(oxalate)⁺ complexes in solution (same preparation as described for the tris(oxalato) complex, but 1:2 and 1:1 mixture of the components; data not shown). This strong rhombicity is characteristic for instance for *cis*-bis(oxalato)chromium(III).³⁰

When ascorbic acid was equilibrated with a Cr(oxalate)₃³⁻(δ -Al₂O₃) suspension during 24 h, an analogous ESR signal occurred. It is known that ascorbic acid catalyses the dissociation of oxalate complexes as described by Banerjee et al.^{31,32} Therefore, ESR data in this study indicate that the Cr(III) oxalato complex dissociates and an inner-sphere adsorption complex on the surface of δ -Al₂O₃ with the fragment [Cr(C₂O₄)_x]^{3-2x} ($x = 0, 1, 2$) is formed. Furthermore, the occurrence of the broad ESR signal at $g = 2$ can be interpreted as the inner-sphere surface

- (20) Stünzi, H.; Marty, W. *Inorg. Chem.* **1983**, *22*, 2145.
 (21) Rotzinger, F. P.; Stünzi, H.; Marty, W. *Inorg. Chem.* **1986**, *25*, 489.
 (22) Thompson, M.; Connick, R. E. *Inorg. Chem.* **1981**, *20*, 2279.
 (23) Ichikawa, T.; Miki, H.; Yoshida, H.; Kevan, L. *Surf. Sci.* **1985**, *158*, 658.
 (24) McGarvey, B. R. *J. Chem. Phys.* **1964**, *40*, 809.
 (25) Cornet, D.; Burwell, R. L., Jr. *J. Am. Chem. Soc.* **1968**, *90*, 2489.
 (26) Möhl, W.; Motschi, H.; Schweiger, A. Unpublished data.
 (27) De Biasi, R. S.; Rodrigues, D. C. S. *J. Mat. Sci.* **1981**, *16*, 968.
 (28) Stumm, W.; Hohl, H.; Dalang, F. *Croat. Chem. Acta* **1976**, *48*, 491.
 (29) Staszak, Z. *Spectrosc. Lett.* **1988**, *21*, 981.

- (30) Andriessen, W. T. M. *Inorg. Chem.* **1975**, *14*, 792.
 (31) Das, S.; Banerjee, R. N.; Banerjee, D. J. *Coord. Chem.* **1984**, *13*, 123.
 (32) Banerjee, R. N. *Trans. Met. Chem.* **1985**, *10*, 147.

complex with complete replacement of the oxalate ligands. In this case the same surface coordination is found as for the adsorption of the Cr(III) aquo complex.

The shape of the adsorption isotherm (Figure 5) after a short period of equilibration shows the expected reversal of the slope, i.e. the electrostatic anion adsorption on a positively charged surface. Increasing the equilibration time leads gradually to an inversion of the slope, which becomes stable after ca. 14 days. A comparison with the adsorption isotherm of the aquo complex (Figure 3) shows a smaller slope at 50% of adsorption. Furthermore, a significant shift of the adsorption isotherm to higher pH values is observed. From this it may be inferred that a new cationic surface complex has been formed.

The transition of the intermediate species is further characterized by ESEEM investigations. After 10 min the ESEEM spectrum is structured by the Larmor frequencies of the magnetic nuclei ^{27}Al and ^1H , as indicated by ν_{Al} , $2\nu_{\text{Al}}$, ν_{H} , and $2\nu_{\text{H}}$ (Figure 7). However, the spectrum is still dominated by the modulation of ambient protons resembling the case of $[\text{Cr}(\text{C}_2\text{O}_4)_3]^{3-}$ in solution. Simulation of aluminum ESEEM shows no significant difference for several types of coordination of metal ions to the hydrous oxide surface and gives no clear dependence of the geometrical parameters for various reasons.⁷ The large spin quantum number $I = 5/2$ of ^{27}Al causes the strong aluminum ESEEM, which can also be observed for long distances. Thus for a short equilibration time, the ESEEM spectroscopic data are

indicative of an outer-sphere complex (Chart I) that is also supported by the ESR data (Figure 4).

After 14 days of equilibration time, the ESEEM spectra are dominated by the ^{27}Al frequency ν_{Al} . The broader features in the frequency domain are caused by the fast echo decay (Figure 8). This fast echo decay is interpreted to be due to the increased Cr^{3+} – Cr^{3+} dipolar interactions when inner-sphere surface complexes with $\equiv\text{AlO}$ functional groups are formed at high-density ligand exchange sites. An almost identical echo decay effect has been found for the adsorption of Cu^{2+} on $\delta\text{-Al}_2\text{O}_3$ ⁷ and can be taken as a supplementary evidence for surface complexations. The slow echo decay in Figure 7 on the other hand is indicative of an outer-sphere association; e.g. charge repulsion between Cr^{3+} ions leads to smaller dipolar interactions. The spectra support the finding concluded from the adsorption isotherm that the ligand replacement of $(\text{C}_2\text{O}_4)^{2-}$ has come to an equilibrium. The adsorption isotherm which is different from the one of $\text{Cr}(\text{H}_2\text{O})_6^{3+}$ indicates that a new cationic surface complex has been formed. It is suggested that this surface complex consists of the $[\text{Cr}(\text{C}_2\text{O}_4)_x]^{3-2x}$ ($x = 1, 2$) moiety and the $[\text{Cr}(\text{aq})]^{3+}$ fragment binding to the $\delta\text{-Al}_2\text{O}_3$ surface (Chart II). A bidentate binding is proposed in analogy to previous findings with Cu^{2+} and VO^{2+} ²⁶ on $\delta\text{-Al}_2\text{O}_3$.

Acknowledgment. This work was supported by a grant from the Board of the Swiss Federal Institute of Technology.

Contribution from the Department of Chemistry,
University of Wisconsin—Milwaukee, Milwaukee, Wisconsin 53201

Spectroscopic Evidence for a Centrosymmetric Dithionite Anion in the Solid State: Vibrational Spectroscopy of Tetraethylammonium Dithionite

William C. Hodgeman, Jeffrey B. Weinrach,[†] and Dennis W. Bennett*

Received March 28, 1990

Infrared and Raman spectroscopic studies of tetraethylammonium dithionite reveal that the dithionite anion adopts a staggered centrosymmetric configuration in the solid state, and in solution in both aqueous and nonaqueous solvents. This contrasts markedly with the structure of $\text{S}_2\text{O}_4^{2-}$ in salts containing the dithionite ion in the proximity of a relatively small cation, in which the ion adopts an anomalous "eclipsed" conformation. Moderate differences for lower energy vibrations are noted for $(\text{Et}_4\text{N})_2\text{S}_2\text{O}_4$ in going from the solid state or nonaqueous solvents into aqueous solution. A normal-coordinate analysis of $\text{S}_2\text{O}_4^{2-}$ in $(\text{Et}_4\text{N})_2\text{S}_2\text{O}_4$ resulted in a sulfur–sulfur bond stretch force constant of $1.3 \text{ mdyn } \text{\AA}^{-1}$. The two Raman-active bands at 472 and 208 cm^{-1} consist of approximately equal contributions from the S–S bond stretch and S–S–O valence angle bend internal coordinates. There is no independent vibrational mode dominated by the S–S bond stretch internal coordinate, thus precluding the existence of a "sulfur–sulfur" group stretching frequency.

Introduction

From the time of its discovery in the early 1800s, the structure and chemistry of the common dithionite anion have sparked interest and stimulated debate.¹ On the basis of simple VSEPR considerations, the expected conformation for the $\text{S}_2\text{O}_4^{2-}$ ion should parallel the structures of other known sulfur–oxygen anions containing sulfur–sulfur bonds, such as $\text{S}_2\text{O}_3^{2-}$ and $\text{S}_2\text{O}_6^{2-}$. In the absence of external perturbations, all three ions would be expected to adopt staggered configurations, with $\text{S}_2\text{O}_6^{2-}$ and $\text{S}_2\text{O}_4^{2-}$ belonging to centrosymmetric point groups D_{3d} and C_{2h} , respectively. As illustrated in Figure 1, $\text{S}_2\text{O}_3^{2-}$ and $\text{S}_2\text{O}_6^{2-}$ are "well-behaved" in this respect, with several crystal structures revealing the expected structures² and Raman spectra of their aqueous solutions indicating that the solvated ions are similar to those in the solid state.³ The dithionite ion, however, stands in marked contrast to its cousins. In 1956 Dunitz reported the crystal structure of the disodium salt of the anion. This provided the first crystallographic evidence that it possessed approximate eclipsed C_{2v} symmetry and a sur-

prisingly long sulfur–sulfur distance of 2.39 \AA .⁴ Subsequently, two other crystal structures of the dithionite anion have revealed the same anomalous structure.⁵ The presence of SO_2^- ions in solution and the solid state along with the strong reducing properties of dithionite salts has generally been attributed to this long and apparently weak sulfur–sulfur bond.

Even more striking are the changes that occur in the Raman spectrum of solid $\text{Na}_2\text{S}_2\text{O}_4$ (Figure 2a) when it is dissolved in aqueous solution (Figure 2b). These observations were published separately and independently by Peter and Meyer⁶ and by Takahashi, Kaneko, and Miwa.⁷ On the basis of polarized/depolarized Raman spectra and the mutual exclusion of Raman and

- (1) Berzelius, J. J. *Lehrbuch der Chemie*; Dresden, Germany, 1825; p 472.
- (2) (a) Zachariasen, E. A. *Phys. Rev.* **1932**, *40*, 923. (b) Lindqvist, I.; Morsell, M. *Acta Crystallogr.* **1957**, *10*, 406. (c) Martinez, S.; Garcia-Blanco, S.; Rivoir, L. *Acta Crystallogr.* **1956**, *9*, 145.
- (3) Sato, S.; Higuchi, S.; Tanaka, S. *Appl. Spectrosc.* **1985**, *39*, 822.
- (4) Dunitz, J. D. *Acta Crystallogr.* **1956**, *9*, 579.
- (5) (a) Kiers, C. T.; Vos, A. *Acta Crystallogr.* **1978**, *B34*, 1499. (b) Magnusson, A.; Johansson, L. *Acta Chem. Scand.* **1982**, *A36*, 429.
- (6) Peter, L.; Meyer, B. *J. Mol. Struct.* **1982**, *95*, 131.
- (7) Takahashi, H.; Kaneko, N.; Miwa, K. *Spectrochim. Acta* **1982**, *38A*, 1147.

* To whom correspondence should be addressed.

[†] Current address: Los Alamos National Laboratory, Los Alamos, NM.